Available online at www.elixirpublishers.com (Elixir International Journal)

Crystal Growth

Elixir Crystal Growth 65 (2013) 19724-19730

ISSN: 2229-712X

Electrical and optical characteristic of non-linear optical chalcone derivative

E. D. D'silva[1,*] and S. M. Dharmaprakash[2]

[1]Department of Physics, Center for PG Studies and Research, St. Philomena College, Puttur, 574202, India.
[2]Department of Studies in Physics, Mangalore University, Mangalagangotri, Mangalore 574199, India.

ARTICLE INFO

Article history:
Received: 25 October 2013;
Received in revised form:
25 November 2013;
Accepted: 4 December 2013;

Keywords
Optical materials,
Crystal growth,
Thermogravimetric analysis,
Dielectric properties.

ABSTRACT

Single crystals of (2*E*)-1-(4-bromophenyl)-3-[4-(methylsulfanyl)phenyl]prop-2-en-1-one (4Br4MSP) was grown by slow evaporation solution growth technique at room temperature. The crystal structure of 4Br4MSP was determined using single crystal X-ray diffraction technique and morphology of the crystal was studied. Optical behavior such as UV-vis-NIR absorption spectra and second harmonic generation were investigated to explore the transmission and nonlinear optical (NLO) characteristics of the material. Thermal stability of the sample is confirmed by TGA/DTA analysis. The dielectric and electric properties of the crystal were studied. The laser damage threshold has been measured by using Q-switched Nd:YAG laser and shows good damage threshold value. Crystals were subjected to microhardness study to explore its mechanical characteristic.

Introduction

Chalcone materials are of experimental importance due to their extensive use in biological, chemical, pharmacuitical, and also in non-linear optical field. The second harmonic generation corresponds to second order nonlinearity arises due to the noncentrosymmetric structure of the molecule [1, 2]. The chalcone materials also exhibit third and higher order nonlinear properties when exposed to high energy laser radiation. Higher order nonlinear properties are difficult to utilize in practical applications due to the damage of chalcone material itself, when exposed to high energy laser. Therefore chalcone materials which withstand high energy radiations is also advantages practically. The second and third order properties of chalcone materials have obvious industrial applications in optical communications, optical computing, harmonic generators, frequency mixing, optical switching etc [1, 3].

This paper deals with the synthesis, growth, electrical and optical characterization of 4Br4MSP chalcone derivative. Since it is a noncentrosymmetric crystal, owing to second order NLO properties it has studied extensively in the present investigation. 4Br4MSP is a donor-π-acceptor-π-donor (D-π-A-π-D) type of the molecule and charge transfer is considered to be from donor end to acceptor end of the molecule. And SHG efficiency is found to be greater than that of 3-Br-4'-methoxy chalcone (3BMC, 2 times that of urea) single crystals [4].

Experimental procedure

Chalcone derivatives can be synthesized by Clainsen – Schmidt condensation method [5]. This is a reaction of substituted acetophenone with substituted benzaldehyde in the presence of an alkali. Commercially available 4-bromoacetophenone and 4-methylthiobenzaldehyde were used without further purification. The synthesis of the compound follows literature method [6]. The resulting crude after synthesis reaction was collected by filtration, dried and purified by repeated crystallization from acetone. The schematic representation of the reaction is given in the scheme1.

The growth medium plays a very important role in the growth of good quality crystals. Therefore a suitable solvent should be selected to grow crystals. 4Br4MSP is insoluble in water, moderately soluble in methanol. We found that acetone is the best solvent for this crystal growth. The solution of 4Br4MSP was prepared in acetone. After filtration by using Whatman filter paper, the solution was transferred into a crystal growth vessel. Next it was kept for crystallization by slow evaporation at room temperature (28^{o}C). Good quality crystals were obtained within a week. Figure 1(a) shows the photograph of 4Br4MSP crystal ($5\times2\times2mm^3$). To determine the morphology of the grown crystal, the faces of the crystal were indexed using Enarf CAD-4 diffractometer along with a four circle goniometer [7]. The morphology of 4Br4MSP crystal in the figure 1 (b) shows its well developed faces.

The single crystal X-ray diffraction data was collected on Bruker Kappa Apex using Apex2 software package. The radiation used was graphite monochromated MoK_{α} radiation [8]. From single-crystal XRD studies, it has been found that the compound crystallizes in the monoclinic system with a space group Cc, which is considered as noncentrosymmetric system, thus satisfying one of the basic material requirements for the SHG activity of the crystal.

The UV-Vis-NIR absorption spectrum of the crystals was recorded using a Cary 5E high resolution spectrophotometer, in the wavelength range of 200 to 1100 nm. Crystals with parallel surfaces and thickness of 1mm were used for this purpose.

In order to explore the thermal properties, the powdered sample of the crystal was selected and the analysis was carried out under the nitrogen atmosphere at a heating rate of 10^{o}/min using Perkin-Elemer simultaneous TGA/DTA analyzer.

Agilant 4263B LCZ meter is used to measure the dielectric properties for different frequencies with an applied voltage of 1Vpp and over a temperature range of 30 to 110 degree Celsius. A thin layer of silver paint on both the faces of the pellet was applied and placed in a dry atmosphere to ensure the proper adhesion of the silver paste. The pellet sample was then placed in a cell which consists of a parallel plate capacitor and was enclosed in a resistance heated furnace. The temperature was monitored using a chromel-alumel thermocouple. The

Tele:
E-mail addresses: deepak.dsilva@gmail.com

temperature of the sample was increased by regulating the input power. At each temperature the sample was kept for 15 minutes to attain thermal equilibrium.

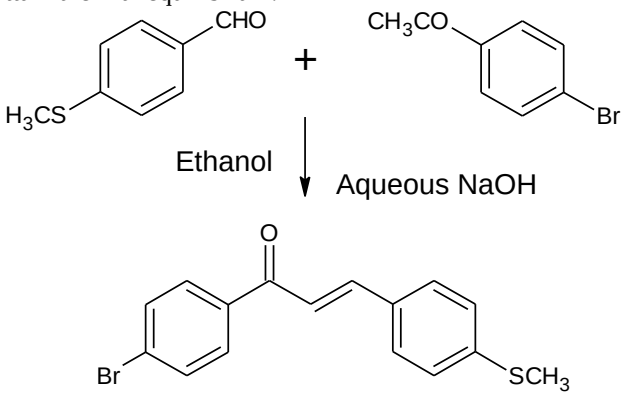

Scheme 1 Synthesis of 4Br4MSP

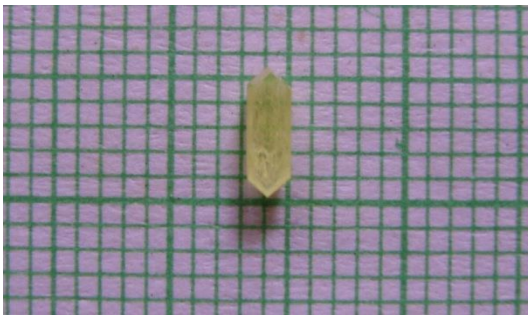

Fig. 1(a) Photograph of the crystal 4Br4MSP

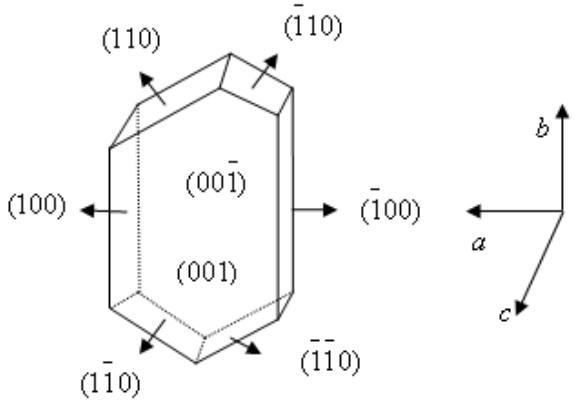

Fig. 1(b) Morphology of the crystal 4Br4MSP

The SHG efficiency was measured in accordance with the powder method developed by Kurtz and Perry using Nd:YAG laser. The tightly packed powdered sample of the crystal was exposed to laser light (of pulse energy 3mJ/pulse, having a wavelength 1064nm, with a pulse width 8ns and repetition frequency 10Hz). The second harmonic wave thus generated from the sample was detected by photomultiplier tube, converted into electrical signal and displayed on the oscilloscope for the measurement of the amplitude of the wave in terms of the volts. The experimental arrangement for laser damage threshold studies consist of a Q-switched Nd:YAG laser, a low power He-Ne laser, a power meter, a beam splitter, and a quartz lens. A suitable beam splitter (50:50) is used to split the laser beam into two parts having equal beam power. One beam was used as reference beam to monitor the laser power and other is focused into the sample using a 15cm lens. A crystal was placed at focus of the lens and the on-axis irradiance was varied in steps of 0.2GW/cm^{2}and the laser beam passed through the crystal was monitored. Damage was checked for an average of 100 laser pulses for fixed on-axis irradiance.

We used Kiethley 2361-V programmable source to study the current-voltage (I-V) dependence of the grown crystals by employing two probe method at room temperature. The better electrical contact was ensured by applying good quality silver paint on both sides of Crystal's pellets. The Kiethley source is kept in resistance mode and current is measured by applying voltage in steps of 2V in the range 0 to 100V.

To estimate the hardness,we selected crystal having flat and smooth surface with the dimension 3x 2x 2mm^3. The selected face was indened gently for different loads with a dwell period of 10 seconds using a research microscope *Climex* for which both Vickers and Knoop indenter are attached.

Results and discussion

Uv-Vis-NIR spectrum

The recorded Uv-Vis-NIR spectrum of the crystal was shown in the figure 2. Usually chalcone crystal show wider transparency range extending into the entire visible and IR region [9]. The cutoff wavelength for this crystal is found to be at about 389nm. Beyond which from visible to IR region there is no prominent absorption peaks. The peak at cutoff wavelength is mainly due to the excitation of C=O group of the molecule. The molecule can be considered for device application, in the region of its transparency.

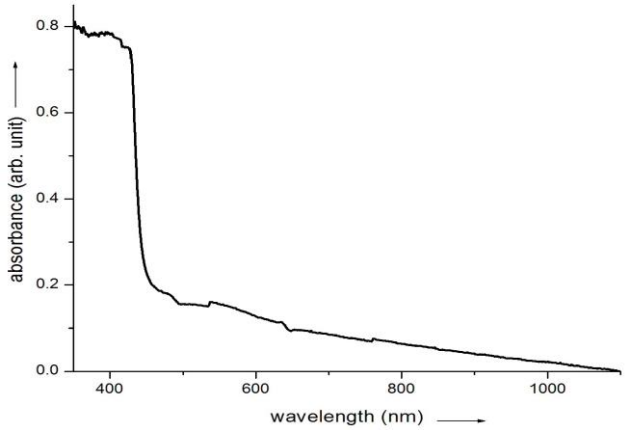

Fig. 2 UV-vis-NIR transmission spectrum of the 4Br4MSP crystal

Optical energy band gap measurements

Optical properties of crystalline materials give information regarding the compound nature and quality of the crystal. In a crystalline material the region of transparency to the electromagnetic radiation defines the intrinsic loss mechanisms and also theoretical transmittance achievable within this region. The transparent spectral region in insulators at short wavelengths is defined by electronic transition across the band gap and at long wavelengths by lattice vibrations. The band gap of the material sets the limiting cut-off wavelengths λ_c defined by $\lambda_c = hc / E_g$. The expression for optical band gap E_g (Tauc's expression) [10], is given by $\omega^2 \varepsilon_2 = (h\omega - E_g)^2$. Where $\varepsilon_2(\lambda)$ is the imaginary part of the complex refractive index, represents optical absorbance and E_g is usually obtained from the plot $\varepsilon_2^{1/2} / \lambda$ vs $(1/\lambda)$. The intersection of the extrapolated spectrum with abscissa gives the gap wavelength λ_g, from which the gap energy is derived to be $E_g = hc / \lambda_g$.

The interpretation of experimental results, viz, the dependence of absorption coefficient α in terms of direct and

indirect transition is most often performed with the help of formula derived for the 3D crystals. Their simplest form as follows

$$\alpha h\nu = A(h\nu - E_g)^r$$, for direct band gap

$$\alpha h\nu = \sum_j A(h\nu - E_g^{'} \pm E_{pj})^r$$, for indirect band gap

Here α is the absorption coefficient, calculated as a function of photon energy. E_g is the energy gap for direct transition, $E_g^{'}$ is the energy gap for indirect transition and E_{pj} is the energy of the phonons assisting the direct transition. *A* and *B* are parameters depending in more complicated way on temperature, photon energy, phonon energy E_p. Specifically the power r=1/2 for direct allowed transition, r=2 indirect, r=3/2 for direct forbidden and r=3 for indirect forbidden transition. The direct band gap can be obtained by plotting $(\alpha h\gamma)^{1/2}$ versus energy (ev). Indirect band gap can be obtained by plotting $(\alpha h\gamma)^2$ versus energy (ev).

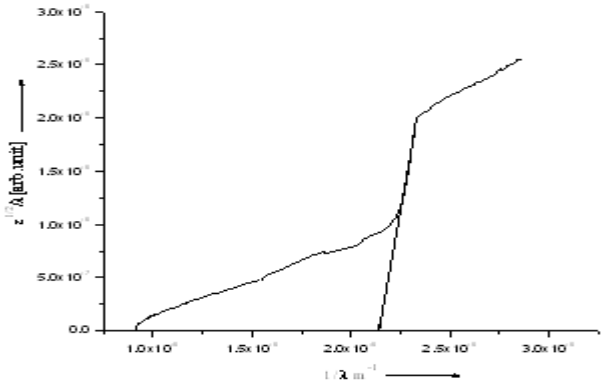

Fig. 3 Plot of $\varepsilon_2^{1/2}/\lambda$ vs $(1/\lambda)$

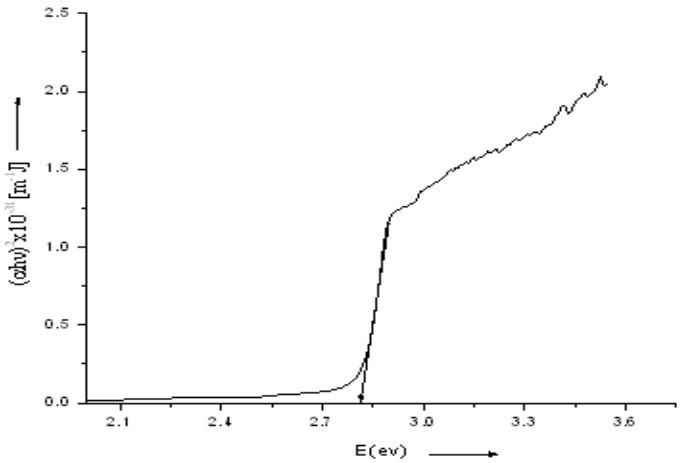

Fig. 4 Plot of $(\alpha h\gamma)^2$ vs E

It is desirable to have low absorption coefficient for NLO materials. The larger the absorption coefficient the more is the dissipation of energy in materials. This causes undesirable thermal effects. The optical energy band gaps for the crystals were calculated using Tauc's expression, direct and indirect band gap expressions. The plots obtained are shown in the figure 3 – 5. The values of band gap energy obtained from the plots $\varepsilon_2^{1/2}/\lambda$ versus $(1/\lambda)$, $(\alpha h\gamma)^{1/2}$ versus E (ev), $(\alpha h\gamma)^2$, versus E (ev) are determined to be 3ev, 2.73ev, 2.81ev respectively. The energy band gap values obtained by employing three different methods are comparable with each other.

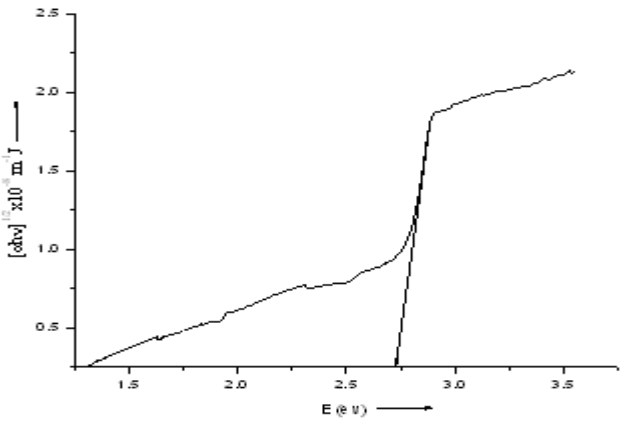

Fig. 5 Plot of $(\alpha h\gamma)^{1/2}$ vs E

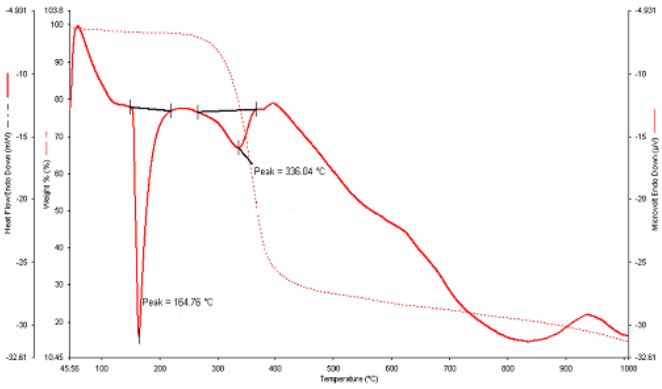

Fig. 6 TGA/DTA curve of the sample

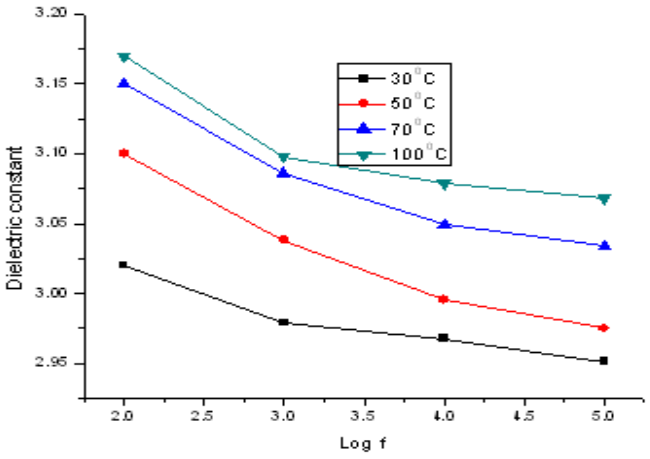

Fig. 7(a) Plot of dielectric constant vs log f for 4Br4MSP

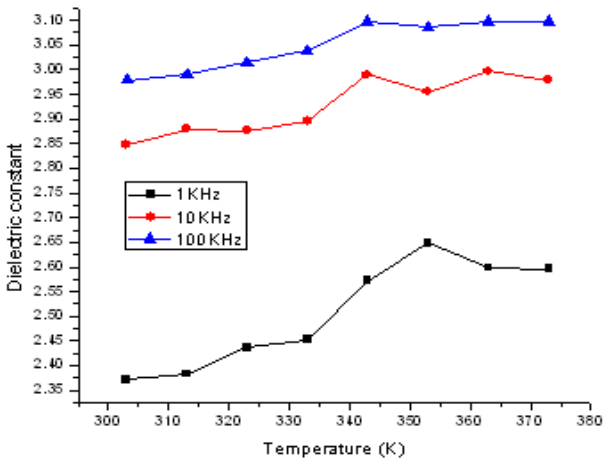

Fig. 7(b) Plot of dielectric constant vs temperature for 4Br4MSP

Thermal studies

Thermo gravimetric analysis (TG/DTA) gives ideas about phase transition temperature, the melting point and the chemical decomposition of the grown crystals. To investigate the thermal stability of the crystal 4Br4MSP, thermo gravimetric analysis was carried out [11].

The results of the analysis are shown in the figure 6. The DTA curve implies that the material undergoes an irreversible endothermic transition where melting begins. The peak of the endothermic represents the temperature 164.76^{o}C at which melting terminates, is corresponding to its melting point. And it is clear that there is no phase transition before melting. The sharpness of the peak shows good crystallinity and purity of the sample. The TG curve of this sample indicates that the sample is stable up to 300^{o}C. The endothermic peak of the DTA at 336.04^{o}C is corresponding to the first phase of the weight loss in the TG curve, indicates decomposition of the sample.

Dielectric properties

The study of dielectric properties is important to understand different polarization mechanisms in solids such as atomic polarization of lattice, orientation polarization of dipoles, space charge polarization, electric and ionic polarization. These polarization effects on the material can be studied by varying dielectric constant as a function of frequency and temperature. This investigation helps in detecting the structural transitions taking place in solids when there are abrupt changes in dielectric properties.

Dielectric constant

Dielectric constant was calculated using the relation $\varepsilon' = Ct/\varepsilon_0 A$, where't' is the thickness, 'A' is the area of the sample. C is the capacitance of the sample, ε_0 is the permittivity of the free space. From the figure 7(a), ε_r (dielectric constant) has high values in the lower frequency regions and then it decreases with the applied frequency. The high value at the low frequencies (100 Hz) may be due to the presence of all four polarizations. And its low value at high frequencies may be due to the loss of significance of these polarizations gradually [12, 13].

From the figure 7(b) it is found that the dielectric constant gradually increases with increase in temperature. The variation of dielectric constant with temperature generally attributed to the crystal expansion, presence of space charge effect in addition to electronic and atomic conduction in the samples. Variation of dielectric constant at low temperature is mainly due to the expansion and electronic and ionic polarization. At higher temperatures, the increase is mainly attributed to the thermally generated charge carriers and impurity dipoles. No abrupt changes are observed in the response indicating the absence of any phase transition. This was confirmed by the thermal studies.

Dielectric loss

Dielectric loss was calculated by the equation $\varepsilon'' = D\varepsilon'$, where D represents the dissipation of the sample at various temperatures. The dielectric loss is the imaginary part of the dielectric constant and determines the loss of energy in the form of heat by a dielectric medium under applied ac field due to the internal friction caused by the switching action of molecular dipoles. Figure 8(a) and 8(b) indicates dielectric loss values decreases with frequency and increases with temperature. The low value of dielectric loss at high frequency in the dielectric loss versus temperature graph indicates that the grown crystals have very low defects [14].

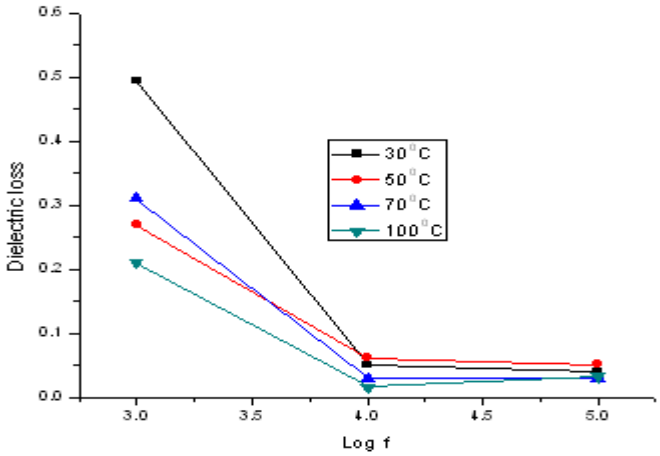

Fig. 8(a) Plot of dielectric loss vs log f at various temperatures

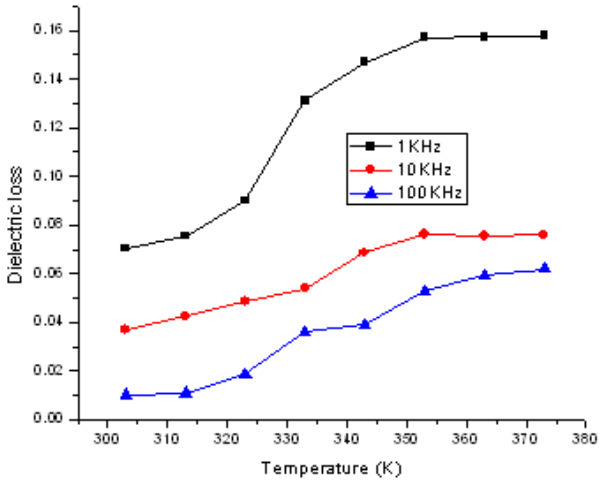

Fig. 8(b) Plot of dielctric loss vs temperature at various frequencies

Specific ac conductance

Specific ac conductance was calculated using relation $Z_{sp} = ZA/t$, where 'A' is area of the parallel planes across which the electric field was applied. 't' is the thickness of the sample. Z represents the specific impedance. The increase in specific impedance with increasing temperature (figure 9(a)) may be attributed to the formation of crystal defects, lowering of barrier height due to the electric field and decrease in density due to thermal expansion. Decrease in impedance with frequency (figure 9(b)) may be attributed to the absence of some kind of polarization at higher frequency [15, 16].

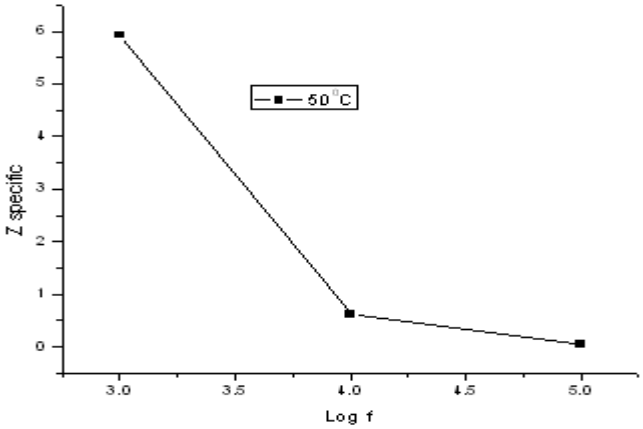

Fig. 9(a) Plot of speific impedance vs log f at 50^{0}C

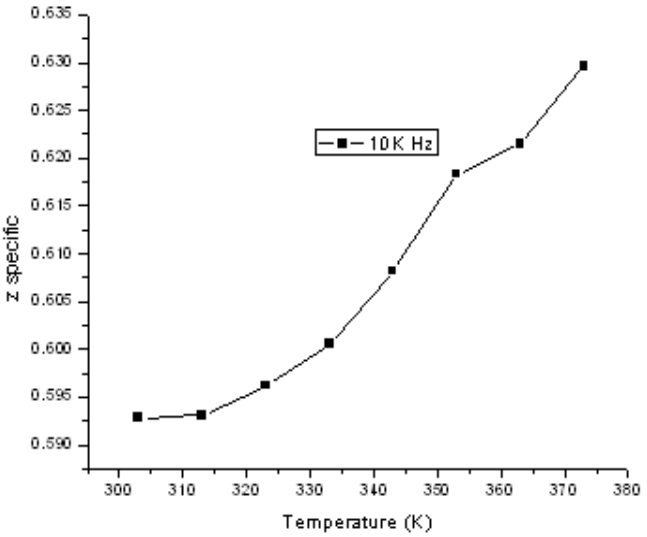

Fig. 9(b) Plot of specific impedance vs temperature at 10KHz

Second harmonic generation

The measurement of SHG efficiency of the 4Br4MSP with the setup analogous to Kurtz method [16] was found to be 3.93 times that of urea crystals with identical particle size. The high value of the SHG reported in the literature was may be due to the presence of impurities or moisture contents in the medium.

Laser damage threshold study

The ability of a crystal to withstand high power laser radiation is one of the important characteristics that any NLO material should possess for high power laser applications. The on-axis irradiance at which the crystal show scattering of laser pulses due to damage produced in the crystal is referred as laser damage threshold of the crystal. The laser damage threshold studies were carried out on solution grown 4Br4MSP single crystals using a Q-switched Nd:YAG laser of pulse width 6ns at a wavelength of 1064nm and a 10Hz repetition rate, operating in TEM_{00} mode, is used as the source. It is observed that 4Br4MSP crystal has laser damage threshold value of 1.2048 GW/cm^2 and this value is found to be comparable with BBO, LAP, urea and other chalcone crystals like MNC, DMMC [4, 18].

Electrical properties

In the case of organic solids, the conductivity due to electrons excited from the valence band to conduction band is negligible. A complex conduction behavior is explained in these materials, which is usually in terms of electrons emitted from the cathode (Schottky-Richardson mechanism) [19] or by electron liberation from the traps in the bulk of the material (Poole-Frankel mechanism) [20]. In our study the current-voltage (I-V) dependence of the grown crystals were conducted using Kiethley 2361-V programmable source measured unit with METRICES-ICS software, by two probe method at room temperature. The current voltage plot of crystal was drawn and resistance of the crystal at room temperature (30^0C) was estimated from the slop of the linear graph, was found to be $1.044X10^{11}$ ohm. The high value of the resistance offered by the crystal indicates that at room temperature it is electrically non-conducting material.

I-V characteristics

Log I versus log V plots for various temperature give rise to straight lines with a voltage dependence of 'I' of the form $I \alpha V^n$, or $I = kV^n$, where 'k' and 'n' are constants [21]. The possibility of ohmic conductions as well as space charge limited conduction is ruled out from the observed behavior of *I–V* characteristics (figure 10). The crystal under study considered to be having defects and the presence of impurity atoms, which cause the scattering of electron waves and rule out the possibility of ohmic conduction. The crystal has low electronic conductivity and this conductivity may also due to the movement of ions in the crystal structure. Naturally with so feeble a charge carrier density, space charge limited conduction seems a remote possibility [22].

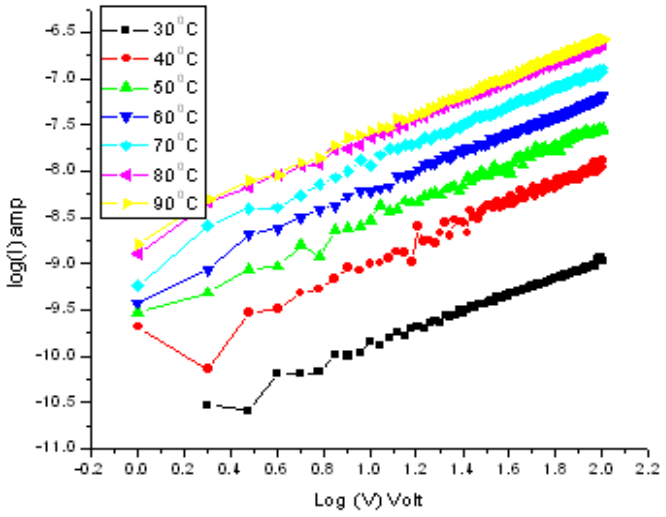

Fig. 10 Plot of log I vs log V for 4Br4MSP

Arrhenius Plots

The conductivity of the material is calculated using the relation $\sigma = d / RA$, d=thickness of sample crystal, A=area of the face of the crystal in contact with electrode [21]. Plots of $\ln(\sigma)$ Vs (1000/T) were drawn. The conductivity values can be fitted to the relation $\sigma = \sigma_0 \exp(-E / KT)$, where E is the activation energy; K is the Boltzmann constant, T represents the absolute temperature and σ_0 is the parameter depending on the material. Activation energy can be estimated from the slop of the above graph using the formula E= - (slope) Kx1000. The plot of $\ln(\sigma)$ Vs (1000/T) for applied 50V is given in the figure 11. The value of activation energy is found to be 0.265ev. The crystal 4Br4MSP has the activation energy value slightly more than reported value of KDP (0.22ev).

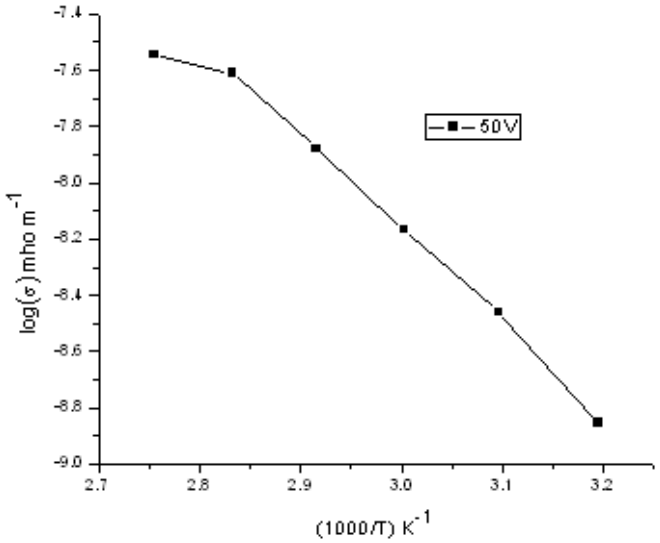

Fig. 11 Arrehenious plots

Microhardness study

Practically hardness measurements give the information of resistance offered by the crystal for localized plastic deformation. Hardness testing is helpful in calculations of mechanical properties like elastic constant, yield strength etc. The most common method of hardness measurements is indentation type. The hardness is estimated from the ratio of the load applied on indenter to the area of the impression left on the specimen. From this, we are expected to get a constant value for hardness at any load. But in practice, load dependence is observed showing higher hardness values at low loads and it decreases as the load is increased, finally becomes load independent. In some cases, though few, a different trend of initial increase of hardness with increase in load then followed by a decrease and finally hardness becoming load independent at higher loads, was also observed [23, 24].

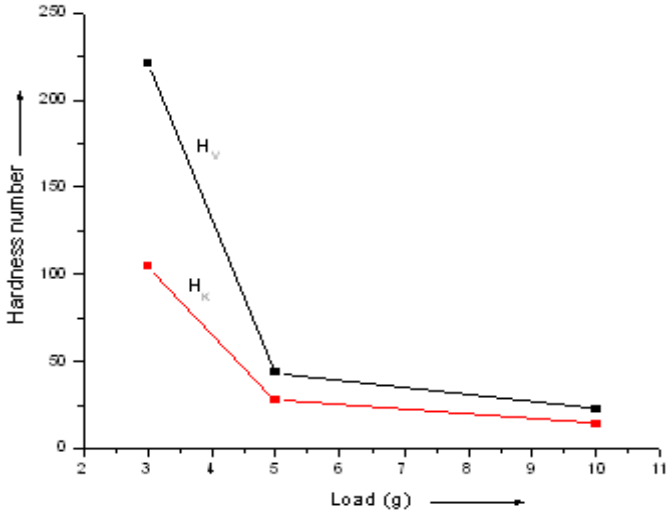

Fig. 12 Variation of H_v and H_k with load

The mechanical studies of chalcone crystals were made by Vickers and Knoop Microhardness tests at room temperature [25]. The crystal 4Br4MSP was mounted properly on the base of the microscope. The indentor orientation is fixed throughout the measurements along a direction with respect to the plane studied. For a particular load, at least five well-defined impressions were considered and the average of all the diagonals (*d*) was considered. The Vickers hardness number (*H*v) was calculated using the standard formula $Hv = 1.8544\ P/d^2$. Where *P* is the applied load in kg, *d* in mm and *H*v is in kg/mm^2. The Knoop indented impressions were approximately rhombohedral in shape. The average diagonal length (d) was considered for the calculation of the Knoop hardness number (Hk) using the relation, $Hk = 14.229\ P/d^2$. Where *P* is the applied load in kg, *d* in mm and *Hk* is in kg/mm^2. Crack initiation and materials chipping become significant beyond 25g of the applied load. The hardness test was carried out for the loads 3g, 5g and 10g. Figure 12, indicates the variation of H_v and H_k as a function of applied load. It can be observed that both values H_v and H_k decreases with increasing load and for further higher loads hardness becomes independent of load.

Conclusion

(2*E*)-1-(4-bromophenyl)-3-[4-(methylsulfanyl)phenyl]prop-2-en-1-one was synthesized and crystals were grown by the slow evaporation method at room temperature. It has a high melting point, when compared to other reported chalcone molecules. The crystal structure is solved by single crystal X-ray diffraction method and the lattice parameters were obtained. UV-vis-NIR result elucidates that the crystal may find useful optical applications in the transparent wavelength window region 390-1100nm. DTA/TGA analysis reveals that material is stable up to the temperature 300^{o}C. The influence of different polarization mechanisms can be understood by measuring the dielectric properties with respect to the frequency and temperature variations. The different electrical conduction methods can be studied by measuring the variation of current and voltage at different temperatures. It is found that crystal is electrically non-conducting at room temperature and this can also be confirmed by the energy gap calculations. The SHG efficiency of the material is 3.93 times than that of Urea. Furthermore laser damage threshold was found to be 1.2048 GW/cm^2 for the wavelength of 1064nm.

Acknowledgements

Authors acknowledge the Department of Science and Technology (DST), Government of India for financial assistance. We are grateful to SAIF Cochin and SAIF Madras for providing experimental facilities. The authors would like to thank, Mr. Deepak, School of Physics, University of Hyderabad, for his help in laser damage studies.

References

[1] Chemla DS, Zyss J. Nonlinear Optical Properties of Organic Molecules and Crystals. New York: Academic Press; 1987.
[2] Huijits RA, Hesseleink GLJ. Chem. Phys. Lett. 1989; 156: 209.
[3] Zyss J. Molecular Nonlinear Optics. Boston: Academic Press; 1993.
[4] Patil PS, Dharmaprakash SM, Ramakrishna K, Fun H-K, Sai Santhosh Kumar R, Narayana Rao D. J.Crystal Growth 2007; 303: 520.
[5] Crasta V, Ravindrachary V, Bhajantri RF, Gonsalves R. J. Crystal Growth 2004; 267: 129-133.
[6] Butcher RJ, Jasinki JP, Yathirajan HS, Narayana B, Mithun A. Acta Cryst. 2007; E63: o3731-o3732.
[7] Levine BF, Bethea CG, Thurmond CD, Lynch RT, Berstein JL. J. Appl. Phys. 1979; 50: 2523.
[8] Zyss J, Nicoud JF, Coquillay M. J. Chem. Phys. 1984; 81: 4160.
[9] D'silva ED, Narayan Rao D, Reji Philip, Ray JB, Rajnikant, Dharmaprakash SM. Journal of Physics and Chemistry of Solids 2011; 72: 824.
[10] Tauc J, Grigorovici R, Vance A. Phys. Stat. Sol. 1966; 15: 627-637
[11] Haines PJ (Eds.). Thermal Analysis Principle; Application and problems. London: Blackie, Academic & Professional; 1987.
[12] Rao KV, Snakula AA. J. Appl. Phys. 1965; 36: 2031.
[13] Narasimha B, Choudhary RN, Rao KV, Mater. Sci. 1988; 23: 1416.
[14] Tareev B. Physics of dielectric materials. Moscow: Mir Publishers; 1979.
[15] Wagner G, Hantemann P. J.Chem.Phys. 1950; 18: 72.
[16] Govinda S, Rao KV. Phys. Stat. Solidi. 1975; 27: 639.
[17] Kurtz SK, Perry TT. J. Appl. Phys. 1968; 39: 3798.
[18] Patil PS, Dharmaprakash SM. J. Crystal Growth 2007; 305: 218-221.
[19] Schottky W. Z. Phys. 1914; 15: 872.
[20] Frenkel J. Phys. Rev. 1938; 54: 647.
[21] Burghate DK, Deshmukh SH, Laxmi Joshi, Deogaonkar VS, Deshmukh PT. Indian Journal of Pure and Applied Physics 2004; 42: 533-538.
[22] Deshmukh SH, Burghate DK, Akhare VP, Deogaonkar VS, Deshmukh PT, Deshmukh MS. Bull. Mater. 2007; 30: 51–56.

[23] Nilam Shah, Dolly Singh, Sejal Shah, Anjum Qureshi, Singh NL, Singh KP. Bull. Mater. Sci. 2007; 30: 477–480.
[24] Sudeshna Mukerji, Tanusree Kar. Metallurgical and Materials Transactions A 2000; 31A: 3089.
[25] Subhadra KG, Kishan Rao K, Sirdeshmukh DB. Bull. Mater. Sci. 2000; 23: 147.